Geoderma 324 (2018) 119–130

Contents lists available at ScienceDirect

Geoderma

journal homepage: www.elsevier.com/locate/geoderma

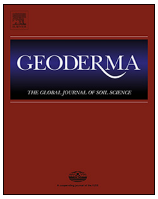

X-ray microtomography analysis of lime application effects on soil porous system

Talita R. Ferreira[a,*], Luiz F. Pires[b,*], Dorthe Wildenschild[c], Richard J. Heck[d], Antonio C.D. Antonino[e]

[a] Physics Graduate Program, Department of Physics, State University of Ponta Grossa, Ponta Grossa, PR, Brazil
[b] Laboratory of Physics Applied to Soils and Environmental Sciences, Department of Physics, State University of Ponta Grossa, Ponta Grossa, PR, Brazil
[c] School of Chemical, Biological, and Environmental Engineering, Oregon State University, Corvallis, OR, USA
[d] School of Environmental Sciences, University of Guelph, Guelph, ON, Canada
[e] Department of Nuclear Energy, Federal University of Pernambuco, PE, Brazil

ARTICLE INFO

Handling Editor: Yvan Capowiez

Keywords:
Soil porous system
3D image analysis
Microtomography
Soil structure
Soil quality

ABSTRACT

Soil liming has demonstrated to be efficient to make acidic soils suitable to agriculture but little research has been done to evaluate its effect on soil structure in the microscale. X-ray microtomography (μCT) is a useful technique to obtain valuable information about the micromorphological characteristics of soil and, thus, can provide important insight into how liming affects such a porous system. In this study, μCT was used to evaluate changes on micromorphological and geometrical properties (porosity, number of pores, pore length, elongation, shape, connectivity and tortuosity) of a soil cultivated under no-tillage system (NTS) caused by the application of lime on the surface. A degraded pasture area representing soil conditions before the NTS implementation was also analyzed. Samples from two soil layers (0–10 cm, A, and 10–20 cm, B) were analyzed with a voxel size of 60 μm. Image visualization, processing and analysis were performed in the Avizo Fire software. Liming improved the soil chemical attributes only at layer A where it also produced positive effects on the soil porous system within a period of thirty months. We highlight the increase in soil porosity and number of pores into which the main soil pore was separated, as evidences of liming effects. At layer A, those pores were found to be more elongated and more connected for the limed site. However, changes in the pattern of the separated pores, with the formation of cylindrical pores in the horizontal orientation for the limed site, were observed at both soil layers, which can be attributed to stimulation of the soil fauna activity due to liming.

1. Introduction

Soil liming is a common agricultural practice to ameliorate important soil chemical attributes related to soil acidity (Turner, 1929). Lime application is also known to promote secondary effects on the soil porous system, which may in turn be reflected as better root and plant development (Haynes and Naidu, 1998). Hence, there has been considerable interest in understanding whether and how this procedure can affect soil processes. In this context, several studies have been focusing on the investigation of liming effects on the soil chemical and physical properties as indicators of changes in soil structure.

Anikwe et al. (2016) and Auler et al. (2017) report that liming has reduced soil bulk density and consequently increased its total porosity. This effect is due to the fact that calcium amendments promote flocculation of soil particles, increasing the porous space in the soil. Carmeis Filho et al. (2016) showed that surface liming reduced the ratio of penetration resistance in the no-till topsoil; the formation of biopores due to biological activity was a result of liming. In the same study, the authors found that liming increased aggregate stability up to a depth of 40 cm and also increased soil macroporosity (equivalent pore diameter ≥ 30 μm) and total porosity to a depth of 10 cm. Based on such results, the authors considered the application of lime as a good strategy to ameliorate the soil structure.

However, conventional studies based on soil physical macro properties often cannot provide detailed information about the possible changes in the soil porous system due to lime application. Data related to the type, number of pores, and their continuity are vital for a better understanding of water retention and movement through the soil profile.

Besides the traditional types of soil analyses, a few scientific contributions have aimed to explore micromorphological analysis techniques to detect liming effects on soil structure. With this purpose, Grieve

---

* Corresponding authors.
E-mail addresses: tali.rf@gmail.com (T.R. Ferreira), luizfpires@gmail.com (L.F. Pires).

https://doi.org/10.1016/j.geoderma.2018.03.015
Received 3 December 2017; Received in revised form 14 March 2018; Accepted 18 March 2018

et al. (2005) quantified the void space of two different horizons of limed and non-limed soil profiles by image analysis of soil thin sections. Those authors found that the percentage of total void space turned out to be greater for the limed soil. The use of soil image analysis, though, presents other advantages such as the possibility of performing a qualitative study of the soil pore space, through which patterns of pore formation can be identified.

Typically, 3D images of samples (of size relevant to soil physics) can be acquired using industrial or synchrotron-based μCT with spatial resolutions varying from 500 μm to 1 μm (e.g. Wildenschild et al., 2002). Usually, with large soil columns and consequently coarse spatial resolutions, it is possible to detect a spatial distribution of large pores, roots, earthworm burrows and cracks. On the other hand, high spatial resolutions can be achieved with samples of a few millimeters in size which allow the evaluation of intra-aggregate porosity and pore-particle interfaces (Vaz et al., 2014). Hence, for each pore domain assessed by a specific spatial resolution, a detailed structural characterization becomes possible.

X-ray μCT has emerged as a very helpful image technique to investigate the internal soil structure (Elliot et al., 2010; Lamandé et al., 2013; Naveed et al., 2013; Pires et al., 2017b). μCT provides 2D radiographs of the linear attenuation coefficient (μ) distributions of the scanned sample. The process of converting μ distributions of a certain material into a reasonable representation of its pore space is done by means of image segmentation (Iassonov et al., 2009; Schlüter et al., 2014). After this procedure, valuable information about micromorphological properties of the soil can be obtained in 2D and 3D. Geometrical properties, such as connectivity and tortuosity of pores can also be assessed by means of 3D images. All these properties allow for a detailed characterization of the spatial configuration of the soil porous system, and cannot be accomplished by the traditional methods.

This study is based on the hypothesis that the application of lime on the surface of a soil cultivated under no-tillage presents positive effects in the soil porous system and, consequently, in its structure. The goal was to use the X-ray μCT technique to investigate soil micromorphological and geometrical properties such as: porosity, number of pores, pore length, elongation, shape, connectivity and tortuosity. Samples from two soil layers (0–10 and 10–20 cm) were analyzed with a resolution of 60 μm.

2. Material and methods

2.1. Soil sampling

The soil samples were collected in a rural site (25°28′S, 50°54′W, 821 m a.s.l.) located in the SE region of the Paraná State, Brazil. The soil was classified as Dystrudept silty-clay (Soil Survey Staff, 2013; Ferreira et al., 2017).

The study was established in May 2012 in a soil under no-till system (NTS) and under pasture, representing the soil conditions before the NTS implementation (REF). Lime rates of 0 (L0) and 20 (L20) t ha^{-1} were applied on the NTS soil surface without disturbing the soil. The lime used had 285 g kg^{-1} of CaO, 200 g kg^{-1} of MgO, 100.6% neutralizing power, 74.7% reactivity, and 75.1% total neutralizing relative power. Two soil layers, 0–10 cm (A) and 10–20 cm (B), were evaluated. Layers A and B will also be referred as top and subsoil layers throughout the text.

A total of 18 undisturbed monoliths (3 samples × 3 treatments × 2 layers) were manually collected (12 × 12 × 12 cm) and posteriorly trimmed to fit dimensions of 8 × 8 × 8 cm. A total of 24 disturbed and undisturbed samples (4 samples × 3 treatments × 2 layers) were also collected for the traditional chemical and physical analyses. The undisturbed samples were collected in steel cylinders (5,0 cm high and 4,8 cm inner diameter), with the help of an Uhland sampler. The sample collection was carried out during bean flowering, thirty months after the liming procedure. The reader is referred to Auler et al. (2017) for a more detailed description of the history of crop rotation adopted for the experiment under study.

2.2. Chemical attributes

Prior to the chemical analysis, the disturbed soil samples were dried in forced air circulation oven (at 40 °C for 48 h) and ground to pass through a 2 mm sieve. Soil organic carbon (OC) was determined by the colorimetric method. Soil pH (active soil acidity) was determined in a 0.01 mol L^{-1} $CaCl_2$ suspension (1:2.5 soil/solution), while the potential acidity (H + Al) was determined by a SMP buffer procedure. Exchangeable Al^{3+} (exchangeable acidity), Ca^{2+} and Mg^{2+} were extracted with 1 mol L^{-1} KCl (1:10 soil/solution), and Al^{3+} was determined by titration with 0.025 mol L^{-1} NaOH solution, and Ca^{2+} and Mg^{2+} by titration with 0.025 mol L^{-1} EDTA (van Raij et al., 2001).

2.3. Image processing and analysis

2.3.1. X-ray CT system and configurations

Prior to the scanning, the cubic shaped samples were dried in a forced air circulation oven (40 °C). A third generation X-ray CT scanner (model NIKON XT H 225 ST, available at the Department of Nuclear Energy, Federal University of Pernambuco, Brazil) was used to scan the samples. The voltage, current and integration time adopted for the image acquisition process were 150 kV, 226 μA and 500 ms. A 0.5 mm Cu-filter was used to minimize beam-hardening effects (e.g. Wildenschild et al., 2002). The soil sample images were generated with a resolution of 60 μm (voxel size: 60 × 60 × 60 μm).

2.3.2. Image reconstruction, processing and analysis

The 3D reconstruction (Table 1) was performed with the software CTPro 3D XT (Nikon Metrology NV). The VGStudio MAX 2.2 (Volume graphics, Heidelberg, Germany) was employed to rescale the reconstructed images to the Hounsfield Scale and to apply the Gaussian filter (radius = 3), exporting them in 16-bit radiometric resolution ($\hat{I}$).

The image visualization, processing and analysis were performed using the commercial Avizo Fire™ software. The data ($\hat{I}$) was denoised with a non-local means filter ($\hat{I}_{NL,}$ search window: 15; local neighborhood: 5; similarity value: 1) (Buades et al., 2005), considering that the Gaussian filter previously applied was not enough to remove noise. Edge enhancement was performed with an unsharp mask ($\hat{I}_{NL+UM}$, edge size: 5; edge contrast: 1; brightness threshold: 0) (Sheppard et al., 2004). The gradient mask (20% standard deviation) was then applied ($\hat{I}_{NL+UM+IG}$) to detect partial volume voxels at phase edges (Schlüter et al., 2014). The chosen parameters for the non-local means filter and unsharp mask were evaluated based on the result of the image gradient mask. Specifically, a lower search window provided coarser phase edges while a higher search window was associated with blur effects.

Methods classified as local segmentation have been reported to provide more satisfying results than the more common global thresholding techniques (Iassonov et al., 2009; Schlüter et al., 2014). To improve the segmentation, a watershed algorithm was used to binarize the images (Vincent and Soille, 1991). A 2nd degree function was fitted to the valley between the peaks corresponding to air and particles in the histogram of $\hat{I}_{NL+UM}$. The minimum (min) was adopted as the approximate gray value which separates the two phases. Therefore, when using the watershed algorithm, the air phase was set from the first value of the histogram to min − 10% and the solid phase was set from

Table 1
Spatial resolution and sizes, in terms of voxels and mm, for the 3D reconstruction of the regions of interest (ROI) within the μCT sample volumes.

Spatial resolution (μm)	ROI (voxels – x, y, z)	ROI (mm – x, y, z)
60	667, 667, 900	40.0, 40.0, 54.0